

SUPPLEMENTARY MATERIAL

Supplementary Figures Legends

Figure S1: Immuno-EM localizes Myo9A expression to glomerular podocytes and tubular epithelia in mouse kidneys. A) negative control; B-D) immunolabeled gold particles (black) localize Myo9A to podocyte foot processes, near slit-diaphragms and GBM (B), to S3 proximal tubular cells (C), to podocyte foot process and cell body (D), often in clusters. Scale bars 500nm.

Figure S2: $Myo9A^{R701X/R701X}$ causes neonatal progressive hydrocephalus. A) Heterozygous p.R701X $Myo9A$ mutant mice ($Myo9A^{R701X/+}$) have no obvious macroscopic brain abnormalities B) Homozygote R701X $Myo9A$ mutant mice ($Myo9A^{R701X/R701X}$) develop severe, progressive hydrocephalus in the first 2 weeks of postnatal life.

Figure S3: Postnatal renal histology in $Myo9A^{R701X}$ mutant mice. A) Representative PAS stain of 2 weeks old homozygous $Myo9A^{R701X/R701X}$ kidneys show poorly organized glomeruli in the outer cortex (insets, x2.5 magnification) and distal nephron dilatation. B) Representative PAS stain of 2 weeks old heterozygous $Myo9A^{R701X/+}$ littermate kidney shows normal histology, glomeruli shown in insets at x2.5 the original magnification. Scale bars =20 μ m.

Figure S4: Podocyte migration assay (wound assay) representative images: *left panels* show wild type podocytes (Wt), *middle panels* show heterozygous (Het) $Myo9A^{R701X/+}$ podocytes, *right panels* show heterozygous $Myo9A^{R701X/+}$ podocytes pre-incubated with Y26732 [10 μ M] for 100 minutes (Het + Y26732). Top images taken at time 0, when the 'wound' was performed, bottom images were taken 16 hours later at x40 magnification.

Table S1: List of all variants shared by proband siblings

GENE	Gene name	Variant	Position	Yale exomes
<i>ACACB</i>	acetyl-CoA carboxylase beta	I464M	464/2458	0
<i>BARD1</i>	BRCA1 associated RING domain 1	R59Q	59/307	2
<i>CDK16</i>	cyclin-dependent kinase 16	P60S	60/570	10
<i>COPG1</i>	coatamer protein complex, subunit gamma 1	D736H	736/874	0
<i>CTBP2</i>	C-terminal binding protein 2	D112A	112/445	30
<i>DHX29</i>	DEAH (Asp-Glu-Ala-His) box polypeptide 29	N841S	841/1369	0
<i>EGFLAM</i> *	EGF-like, fibronectin type III and laminin G domains	Y212X	212/1009	0
<i>ENPP2</i>	ectonucleotide pyrophosphatase/phosphodiesterase 2	V758M	758/888	0
<i>LAMP2</i>	lysosomal-associated membrane protein 2	I252S	252/411	7
<i>MYO9A</i> *	myosin IXA	R701X	701/2548	0
<i>MYZAP</i>	myocardial zonula adherens protein	R352W	352/466	0
<i>NHSL2</i>	NHS-like 2	R832C	832/1225	2
<i>NRK</i>	Nik related kinase	P789S	789/1582	16
<i>PLA2G12A</i>	phospholipase A2, group XIIA	A151T	151/189	0
<i>RABL3</i>	RAB, member of RAS oncogene family-like 3	Y130H	130/236	0
<i>SEC13</i>	SEC13 homolog	C77W	77/322	0
<i>THNSL2</i>	threonine synthase-like 2	X485Q	485/484	0
<i>TOP2B</i>	topoisomerase (DNA) II beta 180kDa	I333T	333/1621	0
<i>TRAPPC13</i>	trafficking protein particle complex 13	T287I	287/412	1
<i>WDR55</i>	WD repeat domain 55	K351E	351/383	0
<i>YTHDC2</i>	YTH domain containing 2	L1133S	1133/1430	0

Asterisks (*) indicate nonsense variants. *EGFLAM*, a gene involved in retinal synapse development not expressed in the kidney that has high LOEUF (0.927), suggesting high tolerance for inactivation, was not selected for evaluation. *MYO9A* has low LOEUF (0.3), suggesting low tolerance for inactivation (<http://gnomad.broadinstitute.org>, last accessed March 12, 2020). Yale exome database from control subjects.^{44,S7}

Table S2: List of 64 FSGS-proteinuria-NS genes genes interrogated in the FSGS-CT cohort

Gene Name	Gene/Protein Description
<i>ACSL4</i>	Acyl-CoA Synthetase Long Chain Family Member 4
<i>ACTN4</i>	Actinin Alpha 4
<i>ALG1</i>	ALG1 Chitobiosyldiphosphodolichol Beta-Mannosyltransferase
<i>ANLN</i>	Anillin Actin Binding Protein
<i>APOE</i>	Apolipoprotein E
<i>APOL1</i>	Apolipoprotein L1
<i>ARHGAP24</i>	Rho GTPase Activating Protein 24
<i>ARHGDIA</i>	Rho GDP Dissociation Inhibitor Alpha
<i>AOX1</i>	Aldehyde Oxidase 1
<i>CD2AP</i>	CD2 Associated Protein
<i>CFH</i>	Complement Factor H
<i>COL4A1</i>	Collagen Type IV Alpha 1 Chain
<i>COL4A3</i>	Collagen Type IV Alpha 3 Chain
<i>COL4A4</i>	Collagen Type IV Alpha 4 Chain
<i>COL4A5</i>	Collagen Type IV Alpha 5 Chain
<i>COQ2</i>	Coenzyme Q2, Polyprenyltransferase
<i>COQ6</i>	Coenzyme Q6, Monooxygenase
<i>COQ8B</i>	Coenzyme Q8B
<i>CRB2</i>	Crumbs Cell Polarity Complex Component 2
<i>CUBN</i>	Cubilin
<i>DGKE</i>	Diacylglycerol Kinase Epsilon
<i>EMP2</i>	Epithelial Membrane Protein 2
<i>EYA1</i>	EYA Transcriptional Coactivator And Phosphatase 1
<i>FAT1</i>	FAT Atypical Cadherin 1
<i>FN1</i>	Fibronectin 1
<i>GFND1</i>	Glomerulopathy With Fibronectin Deposits 1
<i>IFT80</i>	Intraflagellar Transport 80
<i>INF2</i>	Inverted Formin-2
<i>ITGA3</i>	Integrin Subunit Alpha 3
<i>ITGB4</i>	Integrin Subunit Beta 4
<i>KANK1</i>	KN Motif And Ankyrin Repeat Domain-Containing Protein 1
<i>KANK2</i>	KN Motif And Ankyrin Repeat Domain-Containing Protein 2
<i>KANK4</i>	KN Motif And Ankyrin Repeat Domain-Containing Protein 4
<i>LAMB2</i>	Laminin Subunit Beta 2
<i>LAMA5</i>	Laminin Subunit Alpha 5
<i>LMNA</i>	Lamin A
<i>LMX1B</i>	LIM Homeobox Transcription Factor 1 Beta
<i>MTTL1</i>	Mitochondrially Encoded TRNA Leucine 1
<i>MYO1E</i>	Myosin IE
<i>MYH9</i>	Myosin Heavy Chain 9
<i>NEIL1</i>	Nei Like DNA Glycosylase 1
<i>NPHS1</i>	Nephrin
<i>NPHS2</i>	Podocin
<i>NPHS3</i>	Phospholipase C Epsilon 1
<i>NUP93</i>	Nucleoporin 93
<i>NUP107</i>	Nucleoporin 107

<i>NUP205</i>	Nucleoporin 205
<i>NXF5</i>	Nuclear RNA Export Factor 5
<i>PDSS2</i>	Decaprenyl Diphosphate Synthase Subunit 2
<i>PMM2</i>	Phosphomannomutase 2
<i>PODXL</i>	Podocalyxin Like
<i>PLCE1</i>	Phospholipase C Epsilon 1
<i>PTPRO</i>	Protein Tyrosine Phosphatase Receptor Type O
<i>SCARB2</i>	Scavenger Receptor Class B Member 2
<i>SIX1</i>	SIX Homeobox 1
<i>SIX5</i>	SIX Homeobox 5
<i>SMARCAL1</i>	SWI/SNF Related, Matrix Associated, Actin Dependent
<i>SYNPO</i>	Synaptopodin
<i>TRPC6</i>	Transient Receptor Potential Cation Channel Subfamily C Member 6
<i>WDR73</i>	WD Repeat Domain 73
<i>WT1</i>	Wilms Tumor 1 Transcription Factor
<i>XPO5</i>	Exportin 5
<i>ZEB1</i>	Zinc Finger E-Box Binding Homeobox 1
<i>ZMPSTE24</i>	Zinc Metallopeptidase STE24

SUPPLEMENTARY METHODS

WES / Bioinformatics:

We performed whole exome sequencing in two FSGS/proteinuria affected siblings and in 94 DNA samples from the FSGS-CT cohort (ClinicalTrials.gov, NCT00135811) at the Yale Center for Genome Analysis and the Yale DNA Clinical lab.^{21,44,45} Briefly, genomic DNA was isolated from whole blood using Genra Puregene Kit (Qiagen®). Genomic libraries were prepared by standard Illumina protocols and subjected to whole exome capture using capture reagents from Roche or Integrated DNA technologies (IDT®). Exome sequencing was performed on Illumina platforms (HiSeq2000 or NovaSeq6000) with a mean read depth of 80X. Sequence data were aligned to the reference genome using Burrows-Wheeler Aligner (BWA),⁴⁶ analyzed using the Genome Analysis Toolkit (GATK).⁴⁷ Our in-house annotation script that makes use of ANNOVAR⁴⁵ characterized variants for their frequency in public and Yale databases, conservation of mutated positions, prior association with human disease and impact on the encoded protein based on *in silico* prediction software.^{21,23-25,44-47} The variant detection and annotation pipeline have a sensitivity of >95% for single nucleotide changes and 90-95% for small insertions and deletions.⁴⁵ Genotype quality scores and visual analysis of individual chromosomal positions for variants of interest allows exclusion of false variant calls. Sanger sequencing was performed to confirm the *MYO9A* variant in the proband, affected sibling and their parents' genotype.

WES data set from the FSGS-CT cohort was interrogated to identify *MYO9A* variants with population minor allele frequency (MAF) cut off $\leq 0.01\%$ for heterozygous variants and $\leq 0.1\%$ for homozygous and compound heterozygous variants and its predicted impact on protein function. Loss of function variants included truncating, frameshift insertion/deletions and canonical splice site mutations. Cryptic splice site predictions were made using the Berkeley Drosophila Neural Network. Unrelatedness of the cohort samples was established using Plink script.^{S1} The predicted pathogenicity of missense variants was assessed using the bioinformatics scoring of

metaSVM,²³ SIFT²⁴ and CADD²⁵ score and using manual inspection of the conservation of protein residue in orthologues and the predicted functional impact on protein domain involved. Missense variants were classified as predicted-to-be-deleterious if they met deleteriousness criteria using at least two of the three bioinformatics prediction scores of metaSVM, SIFT or CADD score >18. *MYO9A* multiple sequence alignment with base parameters was performed using Clustal Omega-EMBL-EBI (<https://www.ebi.ac.uk/Tools/msa/clustalo/>)^{S2} to assess the phylogenetic conservation of the altered residues identified. Co-segregation of missense variants was not assessed because DNA from the subjects' parents or siblings is not available. A gene panel of 64 known FSGS-causing genes based on the OMIM database (omim.org) and current available literature associated with a phenotype of 'FSGS', 'glomerular proteinuria', 'nephrotic syndrome' at the time of analysis was used to identify relevant variants in the proband siblings and the FSGS-CT cohort samples.

Generation of knock-in *Myo9A*^{R701X} mice

We generated *Myo9*^{R701X} knock-in mice by CRISPR Cas9-mediated gene editing.²⁸ Briefly, the template ssODN (reverse strand): 5'-TTTTCCCAGCTTCCCTGAAAGCAACCACAG CTCTGAAAAATGCTCGAAGAAGTCCCCATCAGAAAACAGCTACAGGATCAATGCCTCA TCCCAGAAACAAAAGCATTCCCTGCTACTTCT-3', including the C>T mutation *MYO9A* p.R701X flanked by ~60 bp *Myo9A* sequence, purified *in vitro* transcribed Cas9 mRNA and *Myo9a* R701 sgRNA (30 ng/μl, 20 ng/μl and 10 ng/μl, respectively) were microinjected into the cytoplasm of C57BL/6J zygotes to achieve heritable gene editing.²⁸ Embryos were transferred to the oviducts of pseudo-pregnant CD-1 foster females using standard techniques following the Yale Genome Editing Center protocols.^{S3-5}

The template for sgRNA *in vitro* transcription (MEGAShortscript kit) was generated by PCR amplification using a primer containing a T7 promoter, a protospacer sequence chosen using

the MIT CRISPR tool <http://crispr.mit.edu>, and the 5' end of the sgRNA scaffold sequence, and the "universal" reverse primer from the pX330 sgRNA expression template (Addgene #42230).²⁸ Cas9 mRNA was transcribed *in vitro* from the pX330 plasmid using the primers listed below. The repair template oligonucleotide (ssODN) containing the specified base change was synthesized by IDT. The C>T change eliminates the PAM and prevents Cas9 re-cleavage of the newly created allele.

Myo9a R701 sgRNA template primer:

5' TGTAATACGACTCACTATAGGATGCTCGAAGAACTGCCCATGTTTTAGAGCTAGA
AATAGC 3'; sgRNA reverse primer: 5' AAAAGCACCGACTCGGTGCC 3'

Cas9FWpX330: 5' TGTAATACGACTCACTATAGGGAGAATGGACTATAAGGACCACGAC 3'

Cas9revpX330: 5' GCGAGCTCTAGGAATTCTTAC 3'

Repair template oligonucleotide (ssODN) (reverse strand):

5' TTTTCCCAGCTTCCCTGAAAGCAACCACAGCTCTGAAAAATGCTCGAAGAACTGCCCAT
CAGAAAACAGCTACAGGATCAATGCCAGTCATCCCAGAAACAAAAGCATTCTGCTACTTC
T 3'

Viable mouse pups were genotyped by sequencing at the Yale Keck facility, using the following primers:

F-5'-TCACCCCCACCATTCAAAC-3'; R-5'-CACACAACAGTAACCCTAAGACG-3'.

A total of 22 pups were born from 3 microinjections: 6 wild type, 6 heterozygous R701X, 5 homozygous R701X and 5 R701 deletion mutant mice. Heterozygous R701X mice were crossed by sibling mating >8 generations to establish a genetically uniform *Myo9A^{R701X}* mutant mouse line from C57BL/6J strain. *Myo9A^{R701X}* knock-in and wild type littermates, male and female, were used from birth to 4 months of age. All animal procedures were performed according to Yale Animal Research Center Animal Care and Use Committee approved protocols.

Urine studies

Spot urine samples were collected from newborn mice and 24h urine collections were obtained from 4 months old mice using metabolic cages. Urine albumin was measured by Albumin Elisa (Bethyl Labs), creatinine was measured by Creatinine Quantitation assay (Bioassay System), following manufacturers' protocols. Urine was resolved by SDS-PAGE after normalizing sample volume to creatinine concentration. Albuminuria was expressed as μg albumin per mg creatinine ($\mu\text{g}/\text{mg}$).

Histology/ IF/ IHC/ ICC

Human kidney biopsy and mouse kidney samples were fixed with 4% paraformaldehyde in PBS at 4°C and embedded in paraffin, placed in 18% sucrose 10 min and embedded in OCT (Sakura) and snap frozen in dry ice-isopentane or processed for TEM. Paraffin sections were stained with periodic acid Schiff (PAS) for histological analysis using light microscopy.⁴⁸⁼⁵² Fluorescent immunohistochemistry was performed in mouse kidney frozen sections and cultured podocytes, respectively. They were fixed with 4% paraformaldehyde in PBS, permeabilized with 0.3% triton-X and blocked with 10% goat serum in PBST and M.O.M® blocking reagent (MKB-2313-1, Vector Laboratories) for 1 hour at room temperature, followed by incubation at 4°C overnight or 2 hours at room temperature with primary antibodies against human MYO9A (mouse monoclonal antibody, clone 4C11, Abnova), podocin (rabbit polyclonal antibody, P0372, Sigma), rabbit anti-laminin (L9393, Sigma), rabbit anti-aquaporin2 (PAS-78809, Invitrogen), rabbit anti-megalin⁴⁹ (MC-220, kindly provided by B. Thomson). Sections were washed and incubated with Alexa Fluor 488 and 594-conjugated secondary antibodies at room temperature for 1 hour. Images were acquired using an Olympus IX71 fluorescence microscope with an Optronics Microfire C camera, PictureFrame™ software and confocal images were obtained using a Leica SP5 Spectral Confocal microscope.

Immunoblot/ Immunoprecipitation

Mouse kidneys were snap frozen in liquid nitrogen at the time of euthanasia, while glomeruli and podocytes were pelleted by centrifugation at the end of culture experiments. Both tissues and cells were lysed in lysis buffer (1% NP-40, 1% Triton X, 50mM Hepes, 150mM NaCl, 0.1 mM EDTA, 0.1mM Neocuproine) for immunoblot and co-immunoprecipitation analysis. Proteins were resolved by SDS-PAGE and transferred to nitrocellulose membranes, which were blocked with 5% dry-milk in TBST, incubated with primary antibodies for MYO9A (mouse monoclonal antibody, clone 4C11, Abnova), actin (rabbit polyclonal antibody, A2066, Sigma), calmodulin (rabbit monoclonal antibody EP799Y, Abcam), GAPDH (mouse monoclonal antibody, 6C5, Millipore), RhoA (rabbit monoclonal antibody, 67B9, Cell Signaling) diluted in blocking buffer, washed and incubated with species specific HRP-conjugated secondary antibodies (Jackson Immuno Research Laboratories Inc.). Immunoblotted proteins were visualized with ECL.⁴⁷ Co-immunoprecipitation was performed as previously described.^{50,51} Briefly, kidney and primary podocyte lysates were pre-cleared with prewashed protein A agarose beads at 4°C for 1 hour, then supernatants were incubated 4 hours at 4°C with anti-MYO9A rabbit polyclonal antibody (A305-702A-M, Bethyl), pre-washed agarose beads were added and incubated overnight. Agarose beads were washed five times in PBS+ protease inhibitors to remove unbound proteins, spun and resuspended in Laemmli sample buffer for western blot analysis.

Quantitative PCR (qPCR)

Total RNA was isolated from kidney and podocytes using TRIzol[®] reagent (Thermo Fisher Scientific). Total RNA (1 µg) from individual mouse kidneys or podocytes (n=3/experimental group) was reverse transcribed to generate cDNA using a using iScript cDNA Synthesis kit (BioRad), amplification was performed using iQ SYBR Green Supermix qRT-PCR master mix (BioRad) and PCR primers designed with NCBI/Primer-BLAST software (U.S. National Library of Medicine, Bethesda, MD) Myo9A primers: (forward) 5'-TCTGAGAAGTAGCAGGAATGC-3'

and (Reverse) 5'-AGCAACCACAGCTCTGAAA-3' with a Bio-Rad CTX, CFX96 Real-time system, C1000 Touch Thermal Cycler. Reactions were performed in duplicate and experiments were repeated three times. Myo9a mRNA expression was normalized to GAPDH mRNA with the $2^{-\Delta\Delta Ct}$ method, as described previously.⁵²

TEM/ Immuno-EM

Kidney tissue samples were fixed with 2% paraformaldehyde, 2.5% glutaraldehyde in 0.1M Na cacodylate buffer at 4°C.²⁷ After fixation, samples were washed in 0.1M sodium cacodylate buffer, post fixed in 1% osmium tetroxide for 1 hour in the dark on ice, washed in distilled water, stained in Kellenberger solution for 1 hour at room temperature, dehydrated in a series of alcohols and propylene oxide solutions, embedded in EMbed 812 (Electron Microscopy Sciences, Hatfield, PA) and polymerized overnight at 60°C. All solutions were supplied by Electron Microscopy Sciences Hatfield, PA. Ultrathin sections were cut at 700Å on a Leica Ultracut UCT (Leica Microsystems Inc.). Sections were stained in 1.5% aqueous uranyl acetate and Reynolds lead stains and imaged on a FEI Tecnai Biotwin (LaB6, 80 kV) transmission electron microscope equipped with a SIS Morada 11 Mpixel CCD camera. Using TEM high-resolution digital images (2000 dpi), the number of foot processes per μm of GBM length was counted, approximately 100-150 foot processes ($\sim 40\text{-}60 \mu\text{m}$ of GBM) were counted per kidney, $n = 3$ per experimental group, as described.^{52,56} Immuno-gold EM was performed in wild type mouse kidney tissue fixed in 3% paraformaldehyde, 0.01% glutaraldehyde in 0.1M cacodylate buffer. Ultrathin cryosections were quenched with 0.5M ammonium chloride, blocked with TBS 0.1%BSA+10% goat serum and incubated overnight with mouse anti-MYO9A primary antibody [1:25]. The secondary antibody was rabbit anti-mouse IgG [1:50] and the gold conjugate was goat-anti rabbit 10nm gold [1:50]. Sections were post-fixed in 2% glutaraldehyde, stained with osmium oxide and uranyl acetate and examined on FEI Tecnai Biotwin (LaB6, 80 kV) TEM.

Primary podocyte isolation and podocyte culture

Podocytes were isolated from wild type and *Myo9A*^{R701X/+} mice, as described⁵⁰ with few modifications.^{53,54} Briefly, kidneys were removed from 7 days old mice, minced and incubated with Collagenase A and DNase (Roche), filtered on 70nm cell strainers (BD Falcon). The filtered solution containing the glomeruli was placed on rat collagen I-coated dishes and cultured in RPMI medium containing 10%FBS, 10mM HEPES, 1mM Na pyruvate, 0.075% NaHCO₃. When cells outgrowing from glomeruli reached 80% confluence, they were trypsinized, washed and filtered through 40nm cell strainers, cultured on collagen I-coated dishes at 37°C. Primary podocytes from 2-3 mice were pooled according to their genotype and passage 1 or 2 podocytes were used for all experiments. Immortalized human podocytes were cultured as described⁴⁶ and their *Myo9A* expression was examined by immunoblotting and IHC as described above.

Myo9A knockdown

Wild type immortalized mouse podocytes (3x10⁵ x well) plated on collagen I- coated dishes and were transfected with *MYO9A* siRNA 100nM (L-006539 (4649) ON TARGET plus, Dharmacon) following manufacturer's protocol using Lipofectamine RNAi Max reagent (Invitrogen), OptiMEM reduced serum medium (Gibco) and podocyte medium without serum or antibiotics and incubated for 6 hours, then serum was added to 10% final concentration. Preliminary experiments testing 40nM -200nM siRNA determined that 100nM resulted in ~50% *Myo9A* knockdown. Untransfected podocytes and podocytes transfected with non-targeting siRNA 100nM (D-001810-10 ON TARGET plus Non-Targeting control pool, Dharmacon) were used as controls. RNA and protein were extracted 48 and 72 hours post-transfection, respectively, for qPCR, immunoblotting and co-IP or podocytes were used for functional assays 72 hours after transfection; n=3-5 independent experiments were performed.

Adhesion assay

Adhesion assays with crystal violet staining were performed as described.⁵³ Briefly, primary podocytes from wild type and *Myo9A*^{R701X/+} mice or immortalized wild type and *Myo9A*^{KD} podocytes were trypsinized and 1×10^4 cells/well were plated on 96-well collagen I coated plates and allowed to attach during 2 hours incubation at 37°C; nonadherent podocytes were then removed by gentle washing with culture medium followed by PBS, attached podocytes were fixed in 1% paraformaldehyde and stained with 0.02% crystal violet solution (V5265, Sigma) for 1 hour at room temperature, washed 5 times in water, and lysed with 2M guanidine hydrochloride while shaking 5 minutes on a micro plate reader (Bio-Rad Model 550), absorbance was read at 575nm. Results are shown from 4 independent experiments comparing wild type, *Myo9A*^{R701X/+} and *Myo9A*^{R701X/+} podocytes pre-treated with 10 μ M Y26732 for 100 minutes or immortalized wild type and *Myo9A*^{KD} podocytes.

Migration assay

Scratch or 'wound' assays were performed as described.⁵⁵ 1×10^5 wild type and *Myo9A*^{R701X/+} primary podocytes or immortalized wild type and *Myo9A*^{KD} podocytes were plated on 35 mm collagen I-coated dishes, cultured overnight, the following day three 'wounds' were made with a 200 μ L pipet tip on each dish and images taken (time 0) at x40 magnification using an Olympus IX71 inverted microscope with an Optronics MicroFire camera and PictureFrameTM version 3.00.30 software; podocytes were cultured for 16 hours, when new images were taken (time 16 h). Migration area was measured using ImageJ (NIH), calculated as 'wound' area (time 0 – time 16 h), expressed in mean pixels \pm SD. Data from >3 independent experiments comparing wild type, *Myo9A*^{R701X/+} and *Myo9A*^{R701X/+} podocytes pre-treated with 10 μ M Y26732 for 100 minutes or immortalized wild type podocytes compared to *Myo9A*^{KD} podocytes, using 2 plates per experimental condition are reported.

RhoA activity

Activated RhoA was measured with a commercial Rho activation pulldown assay kit (Millipore) that uses agarose beads bound to a GST-tagged fusion protein corresponding to residues 7–89 of mouse Rhotekin Rho-binding domain to pulldown and isolate active RhoA,⁵⁶ following the manufacturer's instructions. Briefly, 1mg protein from kidney tissue, isolated glomerular or primary podocyte lysates was incubated with Rhotekin RBD-agarose beads for 45 min at 4°C, followed by centrifugation, beads were extensively washed, and supernatants were discarded. The beads were then resuspended in Laemmli buffer, boiled and pelleted to collect the eluate. After the pulldown, eluted active RhoA was detected by immunoblotting using a rabbit monoclonal RhoA antibody (Cell Signaling Technology).⁵⁷ Total RhoA, GAPDH and actin served as loading controls. RhoA activity was calculated as active RhoA/total RhoA obtained from the quantification of 3 independent experiments for each preparation (kidneys, glomeruli and podocytes), genotype and experimental condition.

Supplementary References

- S1. Purcell S, Neale B, Todd-Brown K, et al. PLINK: a tool set for whole-genome association and population-based linkage analyses. *Am J Hum Genet* 2007;81:559–575.
- S2. Madeira F, Park YM, Lee J, et al. The EMBL-EBI search and sequence analysis tools APIs in 2019. *Nucleic Acids Res.* 2019;47(W1):W636-W641. doi: 10.1093/nar/gkz268.
- S3. Ran FA, Hsu PD, Wright J, et al. Genome engineering using the CRISPR-Cas9 system. *Nat Protoc* 2013;8:2281-2308.
- S4. Ran FA, Hsu PD, Lin CY, et al. Double nicking by RNA-guided CRISPR Cas9 for enhanced genome editing specificity. *Cell* 2013;154:1380-1389.
- S5. Pyzocha NK, Ran FA, Hsu PD, et al. RNA-guided genome editing of mammalian cells. *Methods Mol Biol* 2014;1114:269-277.
- S6. Veron D, Reidy KJ, Bertuccio C, et al. Overexpression of VEGF-A in podocytes of adult mice causes glomerular disease. *Kidney Int* 2010;77:989-999.
- S7. Lemaire, M. Fremeaux-Bacchi V, Schaefer F, et al. Recessive mutations in DGKE cause atypical hemolytic-uremic syndrome. *Nat Genet* 2013;45:531-536.

Figure S1

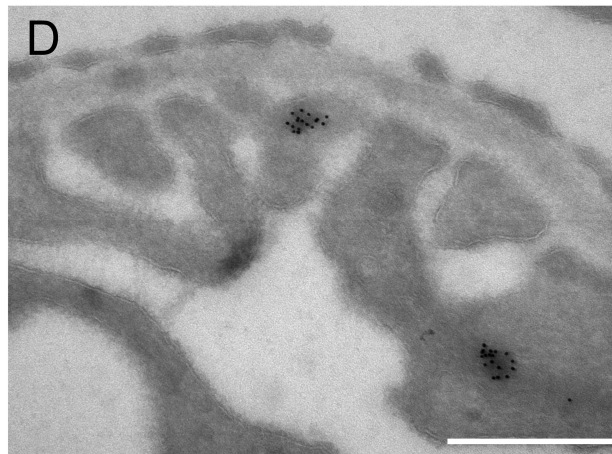
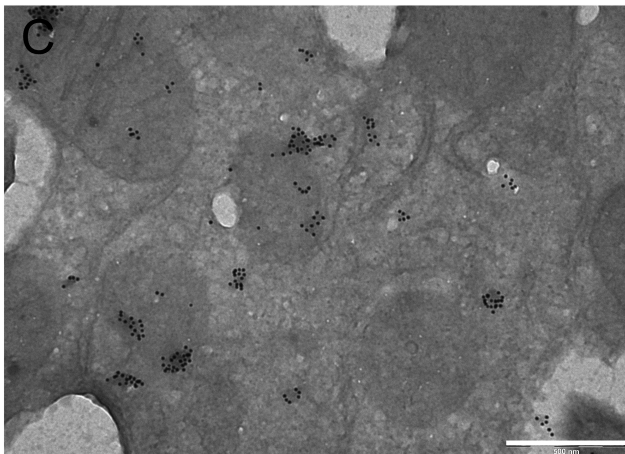
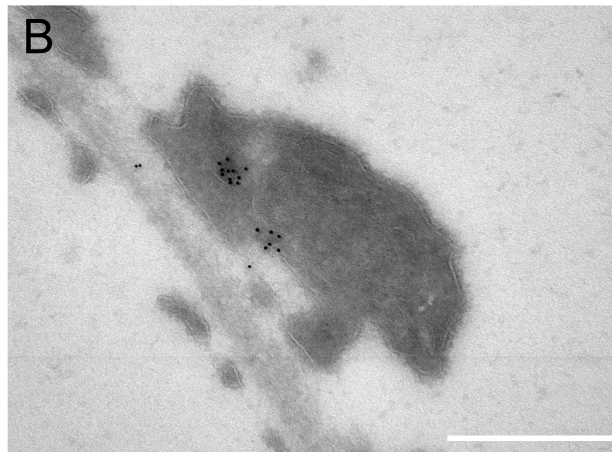
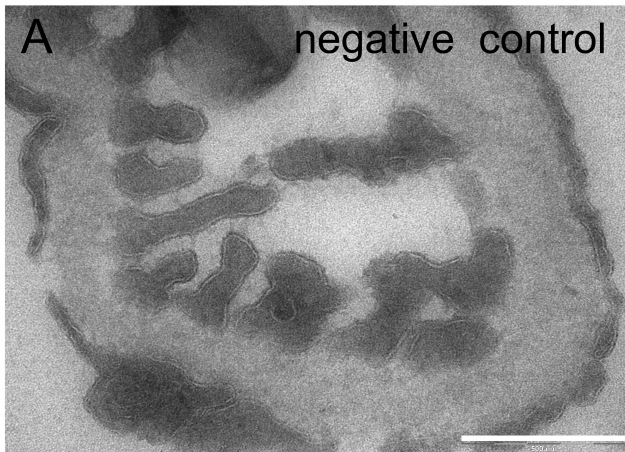


Figure S2

A



B

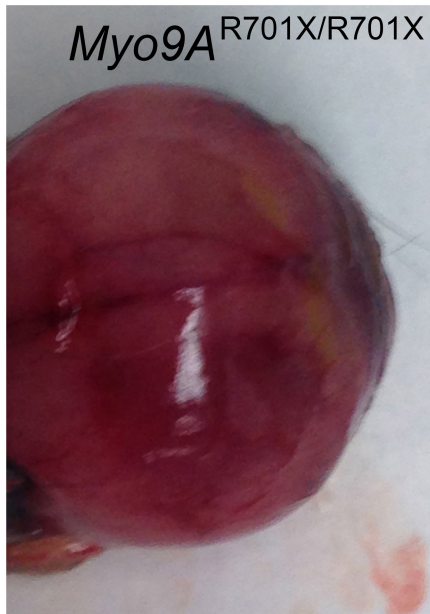


Figure S3

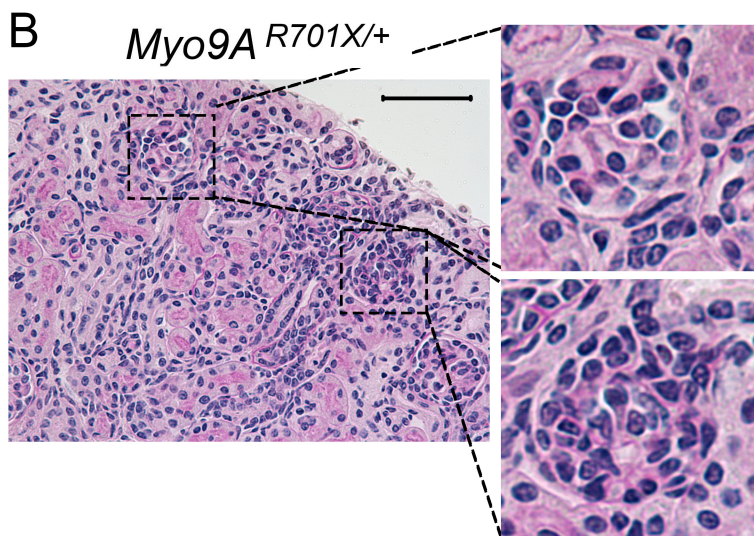
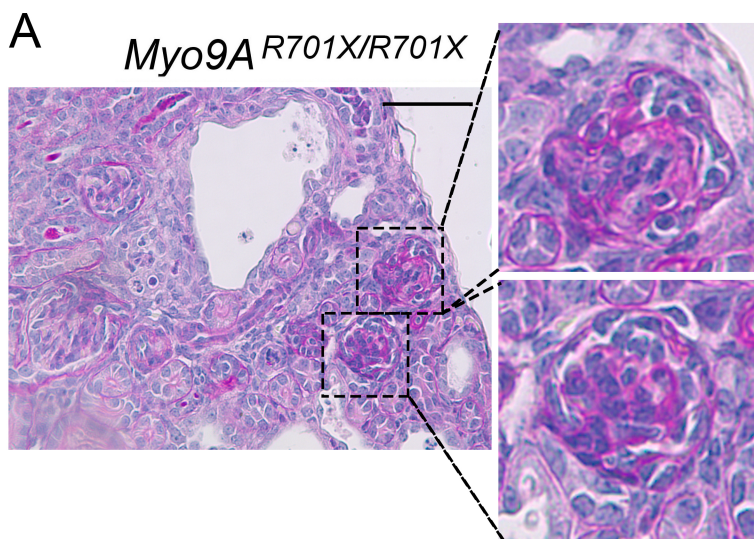


Figure S4

